Dynamics of vacuum impregnation of apples: Experimental data and simulation results using a VOF model

Bruno A.M. Carciofi [a,*], Marc Prat [b], João B. Laurindo [a]

[a] Federal University of Santa Catarina, Department of Chemical and Food Engineering, CP 476, CEP 88040-900, Florianópolis, SC, Brazil
[b] Institut de Mecanique des Fluides de Toulouse, Av. Du Professeur Camile Soula, Toulouse, France

A B S T R A C T

Vacuum impregnation (VI) of foods can be used to accelerate industrial processes. VI consists of removing the air present in a food by applying vacuum and replacing it with a given solution by recovering the atmospheric pressure. In this work, the goal was to study important parameters in the dynamics of VI and to propose a three-dimensional mathematical model (based on the Volume-of-Fluid model) for predicting the impregnation step in apple samples. An experimental device was built for determining the dynamics of VI. It was verified that the capillary radius that allowed for the best representation of the dynamics of vacuum impregnation were in the order of magnitude of micrometers, values that are in the range reported in the literature. The proposed mathematical model showed excellent predictive ability for three-dimensional simulation. However, for more accurate values, one should determine the parameters with improved accuracy.

Keywords:
Mass transfer
Biphasic flow
Porous media
Food processing
Modeling

1. Introduction

Vacuum impregnation (VI) is a method in food processing by which most air and part or all of the native solution are removed from the food porous space (vacuum step) and replaced by an external solution (impregnation step) (Fito, 1994; Laurindo et al., 2007). In the vacuum step, the food is immersed in a solution and exposed to subatmospheric pressure, removing the air trapped in the food porous space. Subsequently, atmospheric pressure is reestablished and the external solution penetrates the food porous space, compressing the residual gas until the pressure equilibrium is reached (Fito, 1994; Fito et al., 1996).

This method implies both a fast change in the food composition and shorter diffusive paths modifying the conditions that control the mass transfer. VI can be useful to introduce dissolved or dispersed substances directly into the porous structure of the food matrix in processes in which solid–liquid operations are present: salting, osmotic dehydration, oil extraction by liquid solvents, incorporation of additives into foods, and others (Andrés 1995; Martínez-Monzó et al., 1998; Barat et al., 2001; Chiralt et al., 2001; Betoret et al., 2003; Mujica-Paz et al., 2003a,b; Laurindo et al., 2007; Schmidt et al., 2008; Martínez-Valencia et al., 2011).

Fito et al. (1996) obtained experimental data of VI dynamics in an apparatus which employed an electronic balance to measure the net mass (or force). However, the balance includes also the mass of the water that evaporates during the VI process and the initial mass of the system, requiring a separate test to measure the water mass that evaporates during the VI experiment. Laurindo et al. (2007) presented a modified device with a load cell instead of electronic balance with the advantage of not requiring the determination of the water evaporated in a separate experiment, which increases the accuracy of the results. Moreover, the electronic interface is placed outside the vacuum chamber and does not suffer influence of the vacuum condition. The load cell system is more flexible, can be easily replaced by another one with a different capacity, and is also accurate for the determination of the time needed to produce degasification (vacuum step) and impregnation of foods submitted to the VI process, even under non-isotonic condition, as shown by Schmidt (2006), Laurindo et al. (2007), Schmidt et al. (2008) and Carciofi (2009).

Fito and Pastor (1994) and Fito et al. (1996) proposed a mathematical model for the equilibrium state in VI processes in porous foods, called by the authors the hydrodynamic mechanism (HDM) coupled with the deformation-relaxation phenomena (DRP). In the HDM model, the impregnated volumetric fraction (X_L) of a food was modeled as a function of the macroscopic pressure gradients imposed, the capillary forces, and the food's effective porosity (ε_e, defined as the fraction of the food's total volume that is occupied by gas). In biological materials, the pressure gradients leads to gas/liquid flows and to a probable deformation of the solid matrix. The DRP model takes into account the deformations of the food matrix in both impregnation steps, by considering the food matrix a viscoelastic material.

* Corresponding author. Tel.: +55 48 3721 6408; fax: +55 48 3721 9687.
E-mail address: bruno@enq.ufsc.br (B.A.M. Carciofi).

http://dx.doi.org/10.1016/j.jfoodeng.2012.05.023

Nomenclature

Abbreviations

DRP	deformation–relaxation phenomena
FCT	Flux-Corrected Transport
HDM	hydrodynamic mechanism
VI	vacuum impregnation
VOF	Volume-of-Fluid

Symbology

a_w	water activity
F_n	net force registered by a load cell, N
F_{no}	net force registered by a load cell at the beginning of the VI process, N
F_{n1}	net force registered by a load cell at the end of the vacuum step, N
F_{n2}	net force registered by a load cell at the end of the VI process, N
g	gravity acceleration, m s^{-2}
$\mathbf{g}$	gravity acceleration vector, m s^{-2}
K	permeability, m^2
GB	gain determined by a balance, kg kg^{-1}
GC	gain determined by a load cell, kg kg^{-1}
$\bar{M}$	average molar mass of the gas phase, kg mol^{-1}
M_b	rigid rod and perforated box mass, kg
M_d	liquid mass drained from the sample during the VI process, kg
M_s	sample mass, kg
M_{so}	sample mass before the VI process, kg
M_{s1}	sample mass at the end of the vacuum step, kg
M_{s2}	sample mass after the VI process, kg
$\mathbf{n}$	normal vector of the liquid interface (non-dimensional)
P_1	vacuum pressure, Pa
P_2	atmospheric pressure, Pa
P_c	capillary pressure, Pa
P_G	pressure at gas phase, Pa
P_k	pressure at k phase, where k = L, G (L = liquid, G = gas), Pa
P_L	pressure at liquid phase, Pa
P_L^*	corrected pressure at liquid phase, Pa
R	universal gas constant, J mol^{-1} K^{-1}
R_c	capillary radius, m
t	time, s
T	temperature, K
$\mathbf{U}_G$	velocity vector for gas phase, m s^{-1}
$\mathbf{U}_k$	velocity vector for k phase, where k = L, G (L = liquid, G = gas), m s^{-1}
$\mathbf{U}_L$	velocity vector for liquid phase, m s^{-1}
$\mathbf{U}_\Gamma$	velocity vector for interface, m s^{-1}
V_b	rigid rod and perforated box volume, m^3
V_s	sample volume, m^3
V_{so}	sample volume before the VI process, m^3
V_{s2}	sample volume after the VI process, m^3
X_L	sample impregnated volumetric fraction, m^3 m^{-3}
X_{La}	apparent sample impregnated volumetric fraction, m^3 m^{-3}
X_{Le}	effective sample impregnated volumetric fraction, m^3 m^{-3}
ε	porosity, m^3 m^{-3}
ε_e	effective porosity, m^3 m^{-3}
θ	contact angle, rad
γ	irreversible relative sample deformation, m^3 m^{-3}
γ_1	relative sample deformation in the vacuum step, m^3 m^{-3}
μ_G	dynamic viscosity for gas phase, Pa s
μ_k	dynamic viscosity for k phase, where k = L, G (L = liquid, G = gas), Pa s
μ_L	dynamic viscosity for liquid phase, Pa s
ρ_a	apparent density of samples, kg m^{-3}
ρ_G	density for gas phase, kg m^{-3}
ρ_k	density for k phase, where k = L, G (L = liquid, G = gas), kg m^{-3}
ρ_L	density of liquid (impregnating solution), kg m^{-3}
ρ_r	real density of samples, kg m^{-3}
σ_{LG}	interfacial tension at liquid–gas interface, N m^{-1}

These models are useful tools for estimating vacuum impregnation, but they do not consider the process dynamics, i.e., they are equilibrium models. Moreover, deformations of the food matrix are not simple to determine experimentally (Laurindo et al., 2007).

Volume-of-Fluid method (VOF) is a model used for simulating the displacement of two or more immiscible fluids in a control volume. As velocities and pressures are assumed to be the same in both fluids, the same set of transport equations is solved for an equivalent fluid. The physical properties of this equivalent fluid are calculated from their volume fractions (Benkenida, 1999; Carciofi, 2009; Carciofi et al., 2011).

With this in mind, the main goal of this work was to study the parameters in the dynamics of the vacuum impregnation process and to propose a three-dimensional mathematical model for predicting the impregnation step. The model is based on the VOF method, and the results are compared with the dynamic experimental data found for vacuum impregnation of apple samples.

2. Material and methods

2.1. Samples

Apple samples (Fuji variety) were used due to the fruit's high porosity (close to 20%), and low deformity (Fito et al., 1996; Laurindo et al., 2007). Fito et al. (1996) reported that apples submitted to vacuum impregnation with isotonic solutions showed relative volumetric expansion of approximately 2.7%. Laurindo et al. (2007) found relative volumetric expansion in samples between 1.8% and 3.1%.

The size of the cylindrical apple samples was 18.0 ± 0.7 mm and 15.1 ± 0.1 mm (length and radius, respectively). Water activity (a_w) of the fresh apples was determined using a hygrometer (Aqualab Model Series 3, Decagon Devices Inc., Pullman, WA, USA) and the apples' water content was determined by drying in an oven at 105 °C until constant weight. Soluble solids content (Brix) in samples was determined by refractive index using a manual optic refractometer (Reichert, model AR200, USA). The apparent (ρ_a) and real (ρ_r) densities of fresh apples were determined by the pycnometric technique as described by Salvatori et al. (1998) using crushed-homogenized-degassed apple samples and an intact portion of apple samples, respectively. Apple porosity (ε) was estimated by Eq. (1). Triplicate determinations were performed for each property

$$\varepsilon = 1 - \frac{\rho_r}{\rho_a} \tag{1}$$

2.2. Impregnating solution

A sucrose/water solution that corresponded to the same water chemical potential (same water activity) of the fresh apple samples

was used in all experiments in order to minimize the diffusive phenomenon. Hence, it was considered that the impregnation of the solution into the samples was caused only due to the macroscopic pressure gradients, i.e., to the spontaneous imbibitions (capillarity phenomenon) and to the flow of solution into the sample when the atmospheric pressure was recovered (imposed pressure gradient).

The sucrose solution concentration (Brix) was measured by refractive index using an optic refractometer (Reichert, model AR200, USA) and the concentration with the same water chemical potential was determined with a calibration curve (a_w as a Brix function), and was equivalent to 19.5 °Brix. The density (ρ_L) of the impregnating solution was determined by picnometry (Lewis, 1993) at 25 °C. Triplicate determinations were performed for each property.

2.3. Experimental setup

A device was built for the measurement of the sample's mass as a function of time during the degasification and impregnation steps, as proposed by Laurindo et al. (2007). A schematic of this device is shown in Fig. 1. It consists of a 50-L vacuum chamber, a vacuum pump (VEB, Model AD230, Germany), and a digital vacuum meter (Motorola, Freescale Semiconductor – MPX2102AP, USA) for online pressure monitoring. Inside the chamber, a single-point load cell (Alfa Instrumentos, model GL1, Brazil), with nominal capacity of 1 kg and readability of 0.1 g, was sustained by a metallic support. A perforated stainless steel cylindrical box was connected to the load cell by a rigid rod with threaded extremities. This system was placed into the vacuum chamber to maintain the food sample immersed in the solution. An electronic interface (Alfa Instrumentos, Model 3102, Brazil) connected the load cell to a computer, allowing for the online recording of the net force variations during the experiments. The force measured by the load cell is the net force, which depends on the mass (weight force) and volume (buoyant force) variations of the system (Fig. 1). The device recorded the changes in the net force (F_n) over time during the whole vacuum impregnation process, as shown in Eq. (2)

$$\frac{F_n}{g} = (M_s + M_b) - \rho_L(V_s + V_b) \quad (2)$$

where g is the acceleration of gravity, ρ_L is the density of the impregnating solution, M_s is the mass of the sample, M_b is the mass of the rigid rod and perforated box, V_s is the volume of the sample, and V_b is the volume of the rigid rod and perforated box immersed in the impregnating solution.

If ρ_L, M_b, and V_b are assumed as constants during the VI, all the changes in F_n during this process are due to changes in V_s (as a consequence of DRP), and in M_s (due to the external solution penetration or native solution drainage). Consequently, both M_s and V_s are dynamic (time-dependent) variables. Volumetric expansions and native solution loss during the vacuum step decrease F_n. Otherwise, the sample impregnation and possible sample shrinking after the reestablishment of atmospheric pressure increase the sample's weight. If the sample is undeformable under vacuum conditions, the only time-dependent variable in Eq. (2) is M_s, and the F_n evolution measured by the load cell directly represents the sample's mass loss (vacuum step) or gain (impregnation step).

The experimental device also allows for controlling the vacuum curves, i.e., the evacuation rate in the vacuum step and the rate of atmospheric pressure recovery in the impregnation step, by means of two solenoid valves (Ascoval, model TLP 584127, Brazil). The first valve was installed on the suction line, between the vacuum pump and the vacuum chamber (on–off operation), and the second one, operating by pulse-width modulation (PWM), was used to allow air to enter the vacuum chamber in order to help controlling the pressure.

2.4. Experimental procedures

Apple samples were weighed, placed inside the perforated box, and submerged into the impregnating solution. For all tests, the sample weight was 65.000 ± 2.500 g, and the vacuum level of 3.3 kPa was applied for 900 s (350 s for reducing the pressure from P_2 to P_1), followed by the impregnation step for 1500 s. In addition, tests with the same system and conditions were performed, without samples or solution, in order to correct possible effects of vacuum on the system. Tests were performed in triplicate.

3. Calculation

3.1. Experimental mass variations

The mass of apple samples before (M_{so}) and after (M_{s2}) the VI process was determined by a semi-analytical balance. The relative mass gain during VI was determined and coded as *GB* (gain determined by a balance), as given by Eq. (3)

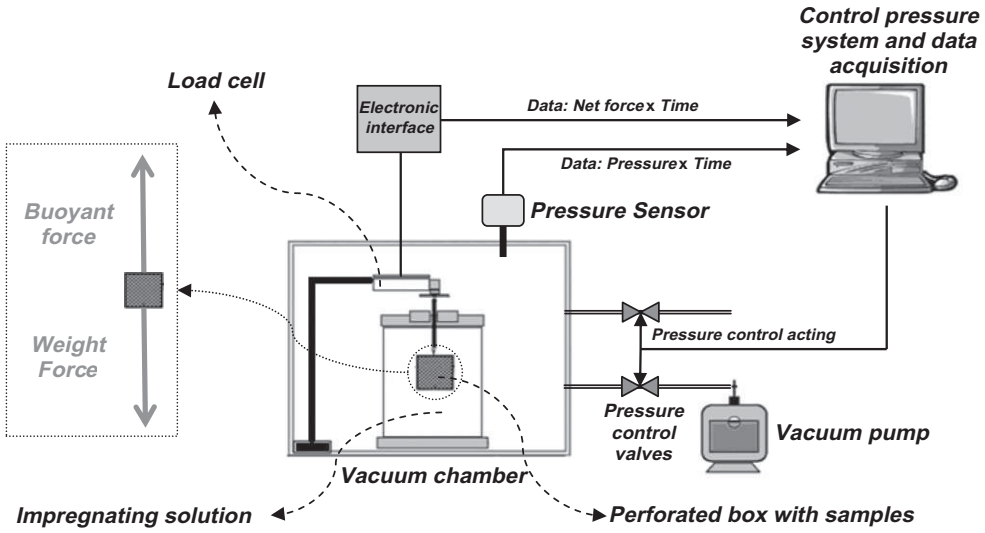

Fig. 1. Schematics of the experimental device used for vacuum impregnation of apples.

$$GB = \frac{M_{s2} - M_{so}}{M_{so}} \tag{3}$$

Similarly, the weight gain values were determined from data registered by the load cell at the beginning (F_{no}/g) and at the end of the VI process (F_{n2}/g), and coded as *GC* (gain determined by a load cell), as shown in Eq. (4). In this case, *GC* does not represent a real mass gain, because the buoyant forces present depend on the possible fruit deformation that leads to volume variation. It is important to mention that the native solution can be drained in the first VI step and replaced by the impregnation solution, and that *GB* and *GC* were calculated in relation to M_{so}

$$GC = \frac{F_{n2} - F_{no}}{gM_{so}} \tag{4}$$

X_L has been estimated by the coupled HDM-DRP model (Fito et al., 1996) as a function of its effective porosity ε_e, the inverse of the compression rate at the relaxation period (defined as the ratio between the sum of the atmospheric pressure, P_2, and capillary pressure, P_c, divided by the pressure applied during the vacuum step, P_1), the relative sample deformation at the end of the vacuum step (γ_1), and the relative sample deformation (γ) observed at the end of the second step (irreversible). The parameters γ_1 and γ are dimensionless and defined as the relative volume variations during the vacuum step and over the whole process of vacuum impregnation, respectively (both volume variations defined from the sample's initial volume). This model is expressed by Eq. (5)

$$X_L - \gamma = \varepsilon_e\left(1 - \frac{P_1}{P_2 + P_c}\right) - \gamma_1\frac{P_1}{P_2 + P_c} \tag{5}$$

In spite of their low deformability (Fito et al., 1996; Salvatori et al., 1998; Laurindo et al., 2007), relative volume variations of apple samples could be determined for different vacuum levels. The value of γ (defined in Eq. (6)) is estimated experimentally from the difference between GB and GC values, as proposed by Laurindo et al. (2007) and given by Eq. (7) (obtained from Eqs. (2)–(4), (and) (6)). The difference is attributed to the irreversible sample deformation that led to buoyant force changes, which modifies the load cell measurement, F_n

$$\gamma = \frac{V_{s2} - V_{so}}{V_{so}} \tag{6}$$

where V_{so} and V_{s2} are the initial and final sample volumes, respectively

$$\gamma = \frac{\rho_a}{\rho_L}(GB - GC) \tag{7}$$

Two experimental values referring to the fraction of the sample impregnated by the external liquid were determined: X_{La}, the apparent volume fraction of the sample impregnated by the liquid, and X_{Le}, the effective volumetric fraction of the sample impregnated by the liquid.

X_{La} was calculated from the ratio between the final and initial sample mass difference and the sample initial volume, as shown in Eq. (8). Alternatively, from Eqs. (3) and (8), X_{La} can be obtained directly from sample and liquid densities and *GB*, as in Eq. (9)

$$X_{La} = \frac{M_{s2} - M_{so}}{V_{so}\rho_L} \tag{8}$$

$$X_{La} = \frac{\rho_a}{\rho_L}GB \tag{9}$$

For calculating X_{Le} by Eq. (10), the mass of the liquid drained during the vacuum step (M_d) was considered as a result of gas expansion inside the sample's porous space (Laurindo et al., 2007; Badillo et al., 2011), as given by Eq. (11)

$$X_{Le} = \frac{(M_{s2} - M_{so}) + M_d}{V_{so}\rho_L} = X_{La} + \frac{M_d}{V_{so}\rho_L} \tag{10}$$

$$M_d = M_{so} - M_{s1} \tag{11}$$

where M_{s1} is the sample weight at the end of the vacuum step.

The value of M_d is given by Eq. (12)

$$M_d = \frac{(F_{no} - F_{n1})}{g} - \gamma_1\frac{\rho_L}{\rho_a}M_{so} \tag{12}$$

where F_{n1}/g is the value obtained from the load cell and γ_1 is the sample's relative deformation, both at the end of the vacuum step (immediately before the recovery of atmospheric pressure).

From Eqs. (3), (10), and (12):

$$X_{Le} = \frac{\rho_a}{\rho_L}GB + \frac{(F_{ro} - F_{r1})}{V_{ao}\rho_L g} - \gamma_1 \tag{13}$$

It is reasonable to assume that during the vacuum step the samples suffered expansion only and that during the impregnation step the samples suffered compression only, as proposed in the HDM-DRP model (Fito et al., 1996). Thus, the value of γ is the difference $\gamma_1 - \gamma_2$, which is generally positive for fruits, as verified by other studies (Fito et al., 1996; Salvatori et al., 1998). Thus, one can conclude that the value γ_1 belongs to the range described by the inequality given by Eq. (14)

$$\gamma \leqslant \gamma_1 \leqslant \frac{(F_{no} - F_{n1})}{gV_{so}\rho_L} \tag{14}$$

The maximum value of γ_1 is the difference of the measurement provided by the load cell at the beginning and at the end of step 1, considering that there is no drainage of fluid during gas expansion ($M_d = 0$). Hence, $X_{Le} = X_{La}$. On the other hand, the deformation at the end of the vacuum step is at least equal to the deformation at the end of the vacuum impregnation, i.e., it is assumed that $\gamma_2 = 0$.

3.2. System modeling

The Eulerian approach proposed by Carciofi et al. (2011) was used to design the system under analysis. The physics and mathematics that describe the impregnation step, i.e., the displacement of a gas by a liquid inside a porous medium, is given by Eqs. (15)–(22). The apple sample was considered an isotropic and homogeneous porous medium represented by an average radius R_c. Other hypotheses were: (a) permeability, temperature, liquid–gas interfacial tension, and porosity were constant; (b) the two fluids are Newtonian and immiscible, and their viscosities are constant; (c) liquid is incompressible; (d) the gas mixture behaves ideally; (e) solid is completely inert; and (f) the pressure relaxation at the gas phase is instantaneous when compared to the interface displacement, implying that the gas density is spatially homogeneous

$$\nabla \cdot \mathbf{U}_k = 0 \tag{15}$$

$$\nabla P_k + \rho_k \mathbf{g} + \frac{\mu_k}{K}\mathbf{U}_k = 0 \tag{16}$$

$$P_G = \rho_G\frac{RT}{\bar{M}} \tag{17}$$

$$P_c = \frac{2\sigma_{LG}\cos\theta}{R_c} \tag{18}$$

$$P_L^* = P_c + P_L \tag{19}$$

$$(P_G - P_L^*)_\Gamma = 0 \tag{20}$$

$$\frac{\mathbf{U}_G}{\varepsilon}\cdot\mathbf{n} = \frac{\mathbf{U}_L}{\varepsilon}\cdot\mathbf{n} = \mathbf{U}_\Gamma\cdot\mathbf{n} \tag{21}$$

$$P_L^* = P_2 + P_c \tag{22}$$

where **U**, P, ρ, μ are, respectively, the velocity vector, pressure, density and the dynamic viscosity defined for liquid (L) or gas (G) phases or at the gas–liquid interface (Γ), **g** is the acceleration vector due to gravity, R is the universal gas constant, T is the system temperature, $\bar{M}$ is the average molar mass of the gas phase, σ_{LG} is the interfacial tension at the liquid–gas interface, θ is the contact angle and **n** is the normal vector of the liquid interface.

A numerical solution of the local balance equations for a Eulerian approach (Eqs. (15)–(22)) can be provide by the homogeneous model, which describes the displacement of two immiscible fluids as a single equivalent fluid (Bonometti, 2005). Therefore, the density and the viscosity of the fluid, defined by the homogeneous model, vary through the interface according to the physical properties of each pure fluid. The VOF (Volume-of-Fluid) model used to simulate the impregnation of a porous medium by a liquid is based on the work of Benkenida (1999), using a phase-indicating function and the conservation of mass and momentum in the liquid and gas phases. This model allows for evaluating the fraction of a gas phase (α_G), the interface position and the fraction of the porous medium occupied by liquid (X_L). The relation between α_G and X_L is given by Eq. (23)

$$X_L = \varepsilon\left(1 - \frac{\int_{V_s} \alpha_G dV}{V_s}\right) \tag{23}$$

3.3. Numerical solution

The numerical solution of the homogeneous VOF model should satisfy at least four conditions: stability, conservation of α_G that leads to local and global mass conservation, positivity of the α_G function, and spatial precision; which reduces the numerical diffusion caused by discontinuity of the α_G function (Benkenida, 1999). This solution was performed by using the Flux-Corrected Transport (FCT) methodology, implemented in JADIM code, developed at the *Institut de Mécanique de Fluides de Toulouse* (IMFT), France.

Initially proposed by Boris and Book (1973), the FCT numerical scheme was modified by Zalesak (1979) to treat numerical diffusion. In the JADIM code, the numerical solution for α_G was obtained by using a displaced grid and the discretization was done by a second-order finite volume method (Magnaudet et al., 1995; Bonometti and Magnaudet, 2007). The pressure field was calculated numerically discretizing by an implicit finite volume method, as presented by Patankar (1980).

3.4. Statistical parameters

MSE (Eq. (24)) and Bias factor (Eq. (25)) were used for comparing experimental data and values calculated by numerical solutions of the homogeneous VOF model

$$\text{MSE} = \frac{\sum(\text{Experimental data} - \text{Numerical values})^2}{\text{Number of data}} \tag{24}$$

$$\text{Bias} = 10^{\frac{\sum \log(\text{Experimental data}/\text{Numerical values})}{\text{Number of data}}} \tag{25}$$

4. Results and discussion

Experimental data on time-force evolution measured by the load cell as a result of variations that occurred on the sample's mass and volume and time-pressure variation on the impregnating chamber containing the perforated box with apple samples are shown in Fig. 2. These results are very representative of the vacuum impregnation of apples investigated in this study. The load cell showed an increase of F_n immediately after sample immersion into the impregnating solution, due to the superficial adherence and a small capillary imbibition. During vacuum application, F_n decreased as a result of both sample deformation and drainage of the native solution present in the apples' intercellular spaces, both promoted by the expansion of gases inside the fruit's porous space.

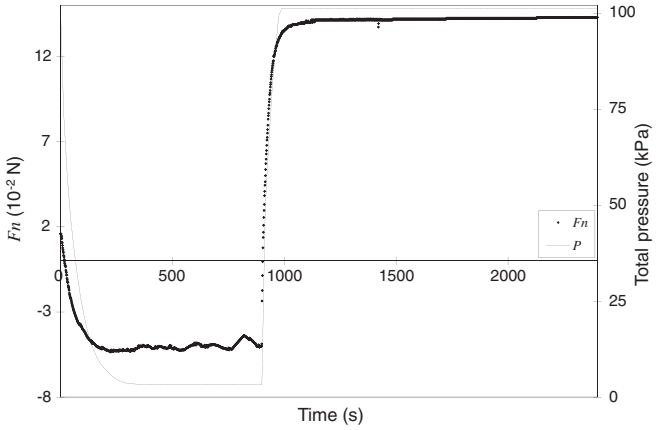

Fig. 2. Evolution over time of the resulting force and total pressure in a typical vacuum impregnation process.

Table 1
Experimental mass and volume variations for apple samples.

Parameter	
GB (kg kg^{-1})	0.253
GC (kg kg^{-1})	0.200
γ (m^3 m^{-3})	0.0417
γ_1 (m^3 m^{-3})	0.0417–0.0848
M_d (kg kg^{-1})	0.000–0.055
X_L (Eq. (5)) (m^3 m^{-3})	0.238–0.240
X_{La} (Eq. (9)) (m^3 m^{-3})	0.199
X_{Le} (Eq. (13)) (m^3 m^{-3})	0.199 a 0.242

The impregnating solution had a density of 1077 kg m^{-3} and concentration of 19.5 °Brix, which guaranteed approximately the same water activity observed for fresh fruit, i.e., 0.988. The apple samples had moisture content of 87.8 ± 1.1% and porosity 0.206 ± 0.006. This value of porosity is in agreement with data reported in the literature for apples, i.e., 0.21 (Karathanos et al., 1996), 0.216 for Red Chef variety (Salvatori et al., 1998), 0.238 for Granny Smith variety (Salvatori et al., 1998), 0.183 for Gala variety (Paes et al., 2007) and 0.205 for Fuji variety (Paes et al., 2008).

Experimental data of relative mass gains (GB and GC), relative deformations (γ_1 and γ), drained mass (M_d), and volumetric fraction of samples impregnated by the external solution (X_{La} and X_{Le}) are shown in Table 1. The difference obtained between GB and GC, as previously mentioned, is credited to the sample's irreversible deformation (swelling), and estimated as 4.17% of the sample's initial volume. This result corroborates the works of Fito et al. (1996), Salvatori et al. (1998) and Laurindo et al. (2007), who observed an increase in fruit volume at the end of the vacuum impregnation processes. Thus, two limit situations can be considered. In the first, assuming that deformation occurred only in the vacuum step, the value γ_1 (which reaches its minimum value) is equal to γ, and if so, M_d reaches its maximum value, i.e., 0.055 kg kg^{-1}. Moreover, considering the other limit condition, in which there was no drainage of native solution ($M_d = 0$), γ_1 reaches its maximum value.

From the coupled HDM-DRP model (Eq. (5)), X_L could be estimated. As the parameters ε, γ, and γ_1 were determined

experimentally, the only unknown parameter was P_c. However, it is easy to demonstrate by Eq. (5) that the variation of P_c between limit values (from zero to ∞) doesn't change the value of X_L significantly. Variations of less than 4.0% are accounted for P_c when its value is the same as P_2, and the maximum error in calculating X_L is below 2.0%. Thus, assuming $P_c = 0$, X_L was calculated for the two limit values of γ_1, as shown in Table 1, obtaining values close to both γ_1.

In comparing the values of the volumetric fraction impregnated by the liquid, the values of X_L were higher than those estimated for X_{La} (approximately 20%). However, X_L is in the range found for X_{Le}, achieving equality between them ($X_L = X_{Le} = 0.240$) for $\gamma_1 = 0.0440$, hence $M_d = 0.052$ kg kg^{-1}. Thus, it would be reasonable to assume that at the end of the vacuum impregnation process, the relative deformation was 4.17% of the sample's initial volume, the drained mass of the native solution was 5.2% of the initial mass, and the fraction of the sample impregnated by the external liquid was 24.0% of the sample's initial volume.

From the homogeneous VOF model, a numerical simulation of the impregnation step (atmospheric pressure recovery) was performed and compared to the experimental data of impregnation of cylindrical apple samples immersed in a sucrose solution. The parameters presented in Table 2 were used in numerical simulation: μ_G and μ_L were obtained from Lide (2004); ε and ρ_L are experimental values; and P_{Go} and P_L are the pressures imposed on the system during the vacuum impregnation process; θ was defined considering the fact that the impregnating solution is a wetting fluid; and σ_{LG} was the value for water at 25 °C (Lide, 2004), although it is known that the addition of carbohydrates may increases the value of water surface tension (Ferreira, 2009). The numerical mesh used was 102 divisions in each spatial coordinate.

The parameters P_c and K should be estimated, respectively, by Eq. (18) and by Kozeny–Carman relation (Eq. (26)), which is adequate for apple tissue as reported by Feng et al. (2004). For its use, the value of Rc (distribution or average value) must be known. Karathanos et al. (1996) reported values of approximately 10–6 m for the capillary radius of dried apple, determined by the mercury porosimetry technique. According to Bazhal et al. (2003a,b) the distribution of the capillary radius of Cortland variety, dried at 45 °C, ranges from 0.008 10^{-6} to 36 10^{-6} m, with average capillary radius of 3.10^{-6} m, determined by mercury porosimetry. Thus, different values of R_c were used in the quest to represent the porous media (apple tissue)

$$K = \frac{(2R_c)^2}{180}\frac{\varepsilon^3}{(1-\varepsilon)^2} \tag{26}$$

Simulations with the homogeneous VOF model and the experimental data from the impregnation step performed with cylindrical apple samples are shown in Fig. 3. This figure presents the simulation results that led to results in agreement with the experimental data. In this way, an effective apple capillary radius was found for apple impregnation. Table 3 lists the statistical parameters MSE and Bias factor corresponding to the simulations that agreed with the experimental data. It was verified that the values assigned to the parameter R_c that allowed for the best representation of the dynamics of vacuum impregnation were in the order of magnitude of micrometers (approximately 1.33 μm), values that are in the range reported in the literature as characteristic of apple pore radius.

Table 2
Parameters employed in VI simulation of cylindrical apple samples.

Parameter	Value	Unit
Numerical grid	102 × 102 × 102	
σ_{LG}	7.2×10^{-2}	N m^{-1}
θ	1.05	rad
P_L	1.01325×10^5	Pa
P_{Go}	3.3×10^3	Pa
μ_G	1.8×10^{-5}	Pa s
μ_L	1.7×10^{-3}	Pa s
ρ_L	1.077×10^3	kg m^{-3}
ε	2.06×10^{-1}	m^3 m^{-3}

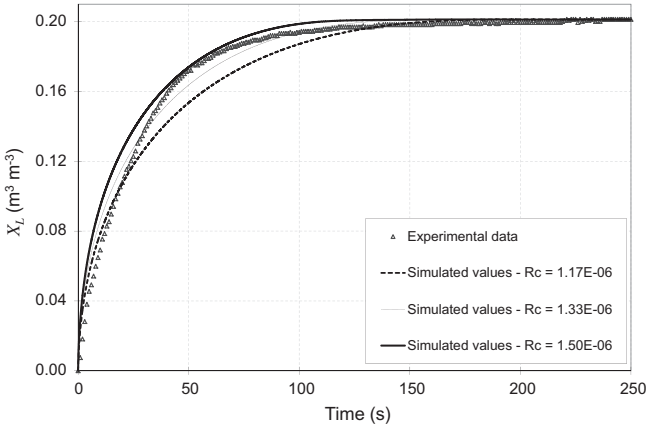

Fig. 3. Experimental data and simulated values of the impregnation step (atmospheric pressure recovery) of cylindrical apple samples.

Table 3
Statistical parameters to compare experimental data and simulated results for VI of cylindrical apple samples.

Capillary radius (10^{-6} m)	MSE	Bias factor
1.00	0.00031	1.07496
1.17	0.00008	1.00628
1.33	0.00004	0.96642
1.50	0.00009	0.93336

The plant tissue is generally a heterogeneous medium, with micrometer-sized intercellular spaces (Karathanos et al., 1996; Bazhal et al., 2003a,b; Mendoza et al., 2007), but cannot be described by a single value of capillary radius. However, hydrodynamically, the assignment of values for R_c represents a quantification of the matrix's potential effects (including the capillary pressure) and flow resistance inside a porous medium, i.e., an effective capillary radius.

In Fig. 3, the homogeneous VOF model overestimates the fraction impregnated at the initial instants. This difference is attributed to the boundary condition imposed on the system during the simulation, which considers a constant pressure on the system boundary equal to the maximum pressure (P_2). However, by observing Fig. 2, one can see that a period of about 90 s between the beginning of the system pressurization and the pressure stabilization at a maximum value was needed. As a result of this higher impregnation rate at the initial instants, the internal pressure gradient (driving force for impregnation) evolves more rapidly in the simulations, resulting in a greater slowdown, underestimating the impregnation rate from the half of this step on. Besides, one should consider that the possible deformations suffered by the sample are not considered in this model.

5. Conclusions

The experimental device proved to be a useful tool in estimating the vacuum impregnation parameters, i.e., relative deformation during the vacuum step, relative deformation at the end of the VI process, and mass of drained solution, normally considered

difficult to determine. Furthermore, the time-resultant force curve as measured by the load cell allows for determining the adequate time required for each VI step. The device also allowed for accurately determining the evolution of the volumetric fraction of the sample, enabling studies of the dynamics of vacuum impregnation as a function of the applied vacuum curve.

The mathematical model proposed for the prediction of the dynamics of VI (liquid penetration into the porous solid) showed excellent predictive ability in three dimensions. In order to obtain more accurate values, one should accurately determine the parameters such as permeability and porous size distribution (influence on the pressure drop and capillary forces). It is still an open problem in Food Engineering, which depends on the use of image-based methods, e.g. tomography, that is expensive and need complex interpretation.

Acknowledgements

The authors thank Dominique Legendre and Annaïg Pedroni for the help on using the JADIM calculation platform, and CNPq and CAPES for the financial support.

References

Andrés, A.M. (1995). Impregnación a Vacio en Alimentos Porosos. Aplicación al Salado de Quesos. Ph.D. thesis, Universidad Politécnica de Valencia, Valencia, Spain.

Badillo, G.M., Segura, L.A., Laurindo, J.B., 2011. Theoretical and experimental aspects of vacuum impregnation of porous media using transparent etched networks. International Journal of Multiphase Flow 37 (9), 1219–1226.

Barat, J.M., Fito, P., Chiralt, A., 2001. Modeling of simultaneous mass transfer and structural changes in fruit tissues. Journal of Food Engineering 49, 77–85.

Bazhal, M.I., Ngadi, M.O., Raghavan, V.G.S., 2003a. Influence of pulsed electroplasmolysis on the porous structure of apple tissue. Biosystems Engineering 86 (1), 51–57.

Bazhal, M.I., Ngadi, M.O., Raghavan, V.G.S., 2003b. Optimization of pulsed electric field strength for electroplasmolysis of vegetable tissues. Biosystems Engineering 86 (3), 339–345.

Benkenida, A. (1999). Développementet validation d'une méthode de simulation d'écoulements diphasiques sans reconstruction d'interface. Application à la dynamique des bulles de Taylor. Ph.D. thesis, Institut National Polytechnique de Toulouse, Toulouse, France.

Betoret, N., Puente, L., Díaz, M.J., Pagán, M.J., García, M.J., Gras, M.L., Martínez-Monzó, J., Fito, P., 2003. Development of probiotic-enriched dried fruits by vacuum impregnation. Journal of Food Engineering 56, 273–277.

Bonometti, T.D. (2005). Développement d'une méthode de simulation d'ecoulements à bulles et à gouttes. Ph.D. thesis, Institut National Polytechnique de Toulouse, Toulouse, France.

Bonometti, T., Magnaudet, J., 2007. An interface-capturing method for incompressible two-phase flows. Validation and application to bubble dynamics. International Journal of Multiphase Flow 33, 109.

Boris, J.P., Book, D.L., 1973. Flux-corrected transport: I. SHASTA, a fluid transport algorithm that works. Journal of Computational Physics 18, 248.

Carciofi, B.A.M. (2009). Dinâmica da impregnação a vácuo de meios porosos. Ph.D. thesis, Universidade Federal de Santa Catarina, Florianópolis, Brazil.

Carciofi, B.A.M., Prat, M., Laurindo, J.B., 2011. Homogeneous volume-of-fluid (VOF) model for simulating the imbibition in porous media saturated by gas. Energy and Fuels 25, 2267–2273.

Chiralt, A., Fito, P., Barat, J.M., Andres, A., Gonzalez-Martinez, C., Escriche, I., Camacho, M.M., 2001. Use of vacuum impregnation in food salting process. Journal of Food Engineering 49 (2–3), 141–151.

Feng, H., Tang, J., Plumb, O.A., Cavalieri, R.P., 2004. Intrinsic and relative permeability for flow of humid air in unsaturated apple tissues. Journal of Food Engineering 62, 185–192.

Ferreira, J.P.M., 2009. Tensão superficial – sua natureza e efeitos. Boletim da Sociedade Portuguesa de Química 93, 43.

Fito, P., 1994. Modeling of vacuum osmotic dehydration of food. Journal of Food Engineering 22, 313–328.

Fito, P., Andrés, A., Chiralt, A., Pardo, P., 1996. Coupling of hydrodynamic mechanism and deformation–relaxation phenomena during vacuum treatments in solid porous food-liquid systems. Journal of Food Engineering 27 (3), 229–240.

Fito, P., Pastor, R., 1994. Non-diffusional mechanism occurring during vacuum osmotic dehydration. Journal of Food Engineering 21 (4), 513–519.

Karathanos, V.T., Kanellopoulos, N.K., Belessiotis, V.G., 1996. Development of porous structure during air drying of agricultural plant products. Journal of Food Engineering 29, 167.

Laurindo, J.B., Stringari, G., Paes, S., Carciofi, B.A.M., 2007. Experimental determination of the dynamics of vacuum impregnation of apples. Journal of Food Science 72, E470–E475.

Lewis, M.J., 1993. Propriedades de los alimentos y de os sistemas de procesado. Ed.Acribia, Zaragoza, Spain.

Lide, D.R., 2004. Handbook of Chemistry and Physics, 84a ed. CRC Press LLC.

Magnaudet, J., Rivero, M., Fabre, J., 1995. Accelerated flows past a rigid sphere or a spherical bubble. Part I: Steady straining flow. The Journal of Fluid Mechanics 284, 97.

Martínez-Monzó, J., Martínez-Navarrete, N., Chiralt, A., Fito, P., 1998. Mechanical and structural changes in apple (var. Granny smith) due to vacuum impregnation with cryoprotectants. Journal of Food Science 63, 499–503.

Martínez-Valencia, B.B., Abud-Archila1, M., Ruiz-Cabrera, M.A., Grajales-Lagunes, A., Dendooven, L., Ovando-Chacón, S.L., & Gutiérrez-Miceli, F.A. (2011). Pulsed vacuum osmotic dehydration kinetics of melon (*Cucumismelo* L.) var. cantaloupe. African, Journal of Agricultural Research, 6(15), 3588–3596.

Mendoza, F., Verboven, P., Mebatsion, H.K., Kerckhofs, G., Wevers, M., Nicolaï, B.M., 2007. Three-dimensional pore space quantification of apple tissue using X-ray computed microtomography. Planta 226, 559–570.

Mujica-Paz, H., Váldez-Fragoso, A., López-Malo, A., Palou, E., Welti-Chanes, J., 2003a. Impregnation properties of some fruits at vacuum pressure. Journal of Food Engineering 56, 307–314.

Mujica-Paz, H., Váldez-Fragoso, A., López-Malo, A., Palou, E., Welti-Chanes, J., 2003b. Impregnation and osmotic dehydration of some fruits: effect of the vacuum pressure and syrup concentration. Journal of Food Engineering 57, 305–314.

Patankar, S.V., 1980. Numerical Heat Transfer and Fluid Flow, first ed. Hemisphere Publishing Corp., New York.

Paes, S.S., Stringari, G.B., Laurindo, J.B., 2007. Effect of vacuum and relaxation periods and solutions concentration on the osmotic dehydration of apples. International Journal of Food Science and Technology 42, 441–447.

Paes, S.S., Stringari, G.B., Laurindo, J.B., 2008. Effect of vacuum impregnation temperature on the mechanical properties and osmotic dehydration parameters of apples. Brazilian Archives of Biology and Technology 51, 779–806.

Salvatori, D., Andrés, A., Chiralt, A., Fito, P., 1998. The response of some properties of fruits to vacuum impregnation. Journal of Food Process Engineering 21, 59–73.

Schmidt, F.C., 2006. Estudo das trocas de massa durante o tratamento de cortes de peito de frango com soluções salinas. Universidade Federal de Santa Catarina, Florianópolis, Brazil, Master in food engineering.

Schmidt, F.C., Carciofi, B.A.M., Laurindo, J.B., 2008. Efeito da impregnação a vácuo na transferência de massa durante o processo de salga de cortes de peito de frango. Ciência e Tecnologia de Alimentos 28, 366–372.

Zalesak, S.T., 1979. Fully multidimensional flux-corrected transport algorithms for fluids. Journal of Computational Physics 31, 335.